EURECOM

Sophia Antipolis

EURECOM
Communication Systems Department
Campus SophiaTech
CS 50193
06904 Sophia Antipolis cedex
FRANCE

Research Report RR-16-325

Novel Half-Duplex Relay Strategy: An LTE implementation

April 30$^{\text{th}}$, 2016
Last update October 20$^{\text{th}}$, 2016

Robin Rajan Thomas, Martina Cardone, Raymond Knopp, Daniela Tuninetti and
Bodhaswar Maharaj

Tel : (+33) 4 93 00 81 00
Fax : (+33) 4 93 00 82 00
Email : {thomas;knopp}@eurecom.fr

Novel Half-Duplex Relay Strategy: An LTE implementation

Robin Rajan Thomas, Martina Cardone, Raymond Knopp, Daniela Tuninetti and
Bodhaswar Maharaj

Abstract

This report presents a practical implementation of a novel two-phase, three-message strategy for half-duplex relaying, which consists of superposition coding and interference-aware cancellation decoding. As opposed to past works, the channel model has a direct link between the source and the destination, through which the source continuously sends information to the destination at a rate close to the capacity of that link. At the same time the source leverages the relay to convey extra information to the destination. With the aim to bridge the gap between theory and practice, this study derives the block error rate with finite block-length and discrete constellation signaling and compares it to the theoretical performance of Gaussian codes with asymptotically large block-lengths. The performance evaluation is carried out on an LTE physical layer compliant simulation test bench. The model assumes a single-antenna source and relay, and multi-antenna destination. During each phase of the transmission, the modulation and coding scheme is adapted to the channel link qualities and selected among those defined by the 3GPP LTE standard.

First the non-fading/static Gaussian additive noise channel is considered. For the case of all single-antenna nodes, the maximum spectral efficiency gap between theory and the proposed practical implementation is of 0.36 bits/dim when the strengths of the source-destination and relay-destination links are the same, and of 0.88 bits/dim when the relay-destination link is $5\,\mathrm{dB}$ stronger than the source-destination link. The performance of the proposed strategy is also compared to a baseline scheme, where there is no physical cooperation between the source and the relay. When the source-destination and relay-destination links are of the same quality, the improvement over the baseline scheme is of 3.45 bits/dim for the single-antenna destination case, and of 3.39 bits/dim for the two-antenna destination case. The fading case is then considered and performance gaps computed as for the static case.

These results confirm once again that physical-layer cooperation and the use of multiple antennas are of critical importance for performance enhancement in broadband wireless systems. More importantly, they show that (i) a practical implementation of high-performing half-duplex relay techniques

for future heterogeneous network deployments is possible with the modulation and coding formats already specified by the 3GPP LTE standard, and (ii) that the gap between theory and practice is small. Optimizing the physical-layer parameters and benchmark its performance against second-order moderate block-length capacity results could potentially show the actual optimality of the proposed two-phase three-message relaying strategy.

Contents

List of Figures

1 Introduction

The benefits of cooperative communications, as a means to enable single-antenna terminals to cooperatively operate with efficiency and diversity gains usually reserved to multi-antenna systems, have been extensively studied [1]. The different cooperative communication techniques and relay strategies available in the literature are largely based on the seminal information theoretic work by Cover and El Gamal [2]. These advances have led to studies of practical relay architectures by 3GPP for inclusion in the LTE Release 9 standard [3, 4].

In this report we provide a practical LTE-based implementation [5] of the novel three-message relay strategy proposed in [6] for the Gaussian Half-Duplex Relay Channel (HD-RC) that is known to be to within a constant gap of the cut-set upper bound on the capacity of the network. The two-phase scheme proposed in [6] employs superposition of Gaussian codebooks at the source, Successive Interference Cancellation (SIC) both at the relay and at the destination, and Decode-and-Forward (DF) at the relay. The channel model has a direct link between the source and the destination, through which the source continuously sends information to the destination at a rate close to the capacity of that link. At the same time the source leverages the relay to convey extra information to the destination at a rate that is, roughly speaking, the minimum capacity of the source-relay (for the relay-listen phase) and relay-destination (for the relay-send phase) links minus the capacity of the source-destination link. The relative duration of the relay-listen and relay-send phases is determined so that the amount of information decoded in the former can be reliably conveyed in the latter. In this work, we first extend the model of [6] to the case of multi-antenna destination and then propose a practical implementation compliant with the LTE standard. A single- and a two-antenna destination, as well as, the Additive White Gaussian Noise (AWGN) and two LTE frequency selective channel models are considered. We bridge theory and practice by showing that low-implementation complexity and high-throughput HD relay schemes are within practical reach for near-future high-spectral efficiency Heterogeneous Network (HetNet) deployments. Moreover, we once again show that enabling physical-layer cooperation among nodes and using SIMO technology is of critical importance in today's and future wireless networks.

1.1 Report Overview

The rest of the report is organized as follows. Section 2 introduces the system model and overviews the scheme proposed in [6], by adapting it to the case when the destination is equipped with multiple antennas. Section 3 presents the simulation test bench. Section 4 evaluates the BLER performance of the proposed scheme for different channel models (AWGN and frequency selective) as well as for the case of single- and two-antenna destination. For all these scenarios, Section 4 compares the achieved spectral efficiency with a baseline scheme that does not allow for direct link source-destination transmission. Both for the AWGN SISO

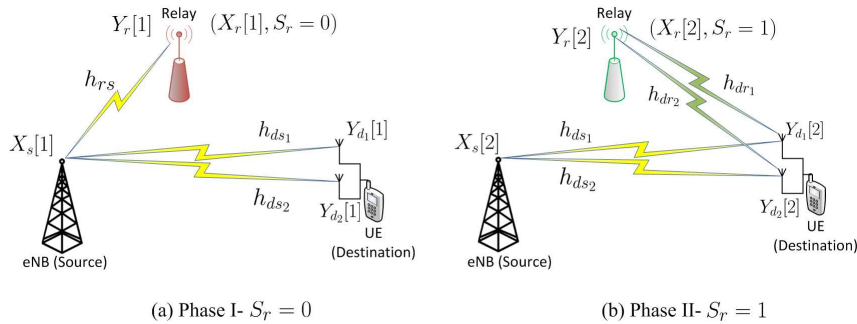(a) Phase I- $S_r = 0$ (b) Phase II- $S_r = 1$

Figure 1: Two-phase relay system model.

and SIMO scenarios, Section 4 also compares the achieved spectral efficiency with the theoretical one. Finally, Section 5 concludes the report.

1.2 Notation

In the rest of the report we use the following notation convention. With $[n_1 : n_2]$ we indicate the set of integers from n_1 to $n_2 \geq n_1$. Lower and upper case letters indicate scalars, boldface lower case letters denote vectors (with the exception of Y^j, which denotes a vector of length j with components $(Y_1, ..., Y_j)$) and boldface upper case letters indicate matrices. With $\mathbf{a}^H$ we indicate the Hermitian transpose of $\mathbf{a}$, with $\mathbf{a}^T$ the transpose of $\mathbf{a}$ and with a^* the complex conjugate of a. $|a|$ is the absolute value of a, $\|\mathbf{a}\|$ is the norm of the vector $\mathbf{a}$ and $|\mathbf{A}|$ is the determinant of the matrix $\mathbf{A}$; $\mathbf{I}_j$ is the identity matrix of dimension j; we use $[x]^+ := \max\{0, x\}$ for $x \in \mathbb{R}$. Logarithms are in base 2.

2 System Model and Transmission Strategy

An HD-RC consists of three nodes: the source, the relay, and the destination. The source has a message $w \in [1 : 2^{NR}]$ for the destination where N denotes the codeword length and R the transmission rate. At time $i, i \in [1 : N]$, the source maps its message w into a channel input symbol $X_{s,i}(w)$ and the relay, if in transmission mode of operation, maps its past channel observations into a channel input symbol $X_{r,i}(Y_r^{i-1})$. At time N, the destination makes an estimate of the message w based on all its channel observations Y_d^N as $\hat{w}(Y_d^N)$. A rate R is said to be ϵ-achievable if, for some block length N, there exists a code such that $\mathbb{P}[\hat{w} \neq w] \leq \epsilon$ for any $\epsilon > 0$. The capacity C is the largest nonnegative rate that is ϵ-achievable for all $\epsilon \in (0, 1)$.

The static/non-fading SIMO Gaussian HD-RC is shown in Fig. 1, where the three nodes are the eNodeB (source), the relay, and the UE (destination), which is equipped with $n_d = 2$ antennas. The input/output relationship is

$$Y_r = h_{rs} X_s (1 - S_r) + Z_r \in \mathbb{C}, \tag{1a}$$

$$\mathbf{y}_d = \mathbf{h}_r X_r S_r + \mathbf{h}_s X_s + \mathbf{z}_d \in \mathbb{C}^2, \tag{1b}$$

where we let $\mathbf{y}_d = \begin{bmatrix} Y_{d_1} & Y_{d_2} \end{bmatrix}^T$, $\mathbf{h}_r = \begin{bmatrix} h_{dr1} & h_{dr2} \end{bmatrix}^T$, $\mathbf{h}_s = \begin{bmatrix} h_{ds1} & h_{ds2} \end{bmatrix}^T$ and $\mathbf{z}_d = \begin{bmatrix} Z_{d_1} & Z_{d_2} \end{bmatrix}^T$. The channel parameters $(h_{ds_i}, h_{dr_i}, h_{rs}), i \in [1 : 2]$ are fixed for the whole transmission duration and assumed known to all nodes (i.e., full Channel State Information (CSI)), the inputs are subject to unitary power constraints, S_r is the switch random binary variable which indicates the state of the relay, i.e., when $S_r = 0$ the relay is receiving while when $S_r = 1$ the relay is transmitting, and the noises form independent white Gaussian noise processes with zero-mean and unit-variance. The model is without loss of generality because non-unitary power constraints or noise variances can be incorporated into the channel gains. It is also worth noting that the scheme designed in this section as well as its derived performance guarantee hold for any value of $n_d \geq 1$. However, we will here focus on $n_d = 2$ as this is the case considered in the practical implementation. For the SIMO Gaussian HD-RC, the following is a generalization of [6, Proposition 5].

Proposition 1. *For the static/non-fading SIMO Gaussian HD-RC the following rate is achievable*

$$R = \log\left(1 + \|\mathbf{h}_s\|^2\right) + \frac{\underline{a}\,[\underline{b}]^+}{\underline{a} + [\underline{b}]^+}, \tag{2a}$$

$$\underline{a} := \log\left(1 + \frac{\|\mathbf{h}_r\|^2 + \|\mathbf{h}_r\|^2\|\mathbf{h}_s\|^2\left(1 - |v|^2\right)}{1 + \|\mathbf{h}_s\|^2}\right), \quad v := \frac{\mathbf{h}_s^H \mathbf{h}_r}{\|\mathbf{h}_s\|\|\mathbf{h}_r\|}, \tag{2b}$$

$$\underline{b} := \log\left(1 + \frac{|h_{rs}|^2}{1 + \|\mathbf{h}_s\|^2}\right) - \log\left(1 + \frac{\|\mathbf{h}_s\|^2}{1 + \|\mathbf{h}_s\|^2}\right). \tag{2c}$$

Moreover, R in (2a) *is to within* 3.51 *bits/dim from the cut-set upper bound to the capacity, irrespectively of the number of antennas at the destination.*

Proof. We give next a sketch of the proof of Proposition 1. The complete proof can be derived by obvious modifications from the proof of [6, Proposition 5].

Codebooks We study a scheme with the following four Gaussian codebooks to transmit three messages:

$$\mathcal{C}_{a1} = \{X_{a1}^{N_1}(w_0) : w_0 \in [1 : M_0]\}, \quad \mathcal{C}_{a2} = \{X_{a2}^{N_2}(w_0) : w_0 \in [1 : M_0]\},$$
$$\mathcal{C}_b = \{X_b^{N_1}(w_1) : w_1 \in [1 : M_1]\}, \quad \mathcal{C}_c = \{X_c^{N_2}(w_2) : w_2 \in [1 : M_2]\},$$

by which we aim to achieve a rate of $R = \frac{\log(M_0 M_1 M_2)}{N_1 + N_2}$ bits/dim. The transmission is divided into two phases: the first phase (i.e., relay receiving) lasts N_1 channel uses, and the second phase (i.e., relay transmitting) lasts N_2 channel uses. In the following, in order to simplify the notation, we omit the length N_1 and N_2 in the superscript of the codewords.

3

Phase I During this phase the relay is listening, i.e., $S_r = 0$ (see Fig. 1(a)). The source selects uniformly at random two messages $w_0 \in [1 : M_0]$ (sent cooperatively with the relay to the destination) and $w_1 \in [1 : M_1]$ (sent directly to the destination). The transmitted signals are

$$X_s[1] = \sqrt{1 - \delta}X_b(w_1) + \sqrt{\delta}X_{a1}(w_0), \tag{3a}$$

$$X_r[1] = 0, \tag{3b}$$

$$\delta = \frac{1}{1 + \|\mathbf{h}_s\|^2}, \tag{3c}$$

where $\delta \in [0, 1]$, which is the scaling parameter that allows for superposition coding, is set as in (3c) for a reason that will become clear in the error analysis (i.e., signals treated as noise should be received at the level of the noise).

The relay applies successive decoding of $X_b(w_1)$ followed by $X_{a1}(w_0)$ from

$$Y_r[1] = h_{rs}\sqrt{1 - \delta}X_b(w_1) + h_{rs}\sqrt{\delta}X_{a1}(w_0) + Z_r[1],$$

which is possible if

$$R_b \leq \gamma \log\left(1 + |h_{rs}|^2\right) - \gamma \log\left(1 + \frac{|h_{rs}|^2}{1 + \|\mathbf{h}_s\|^2}\right),$$

$$R_a \leq \gamma \log\left(1 + \frac{|h_{rs}|^2}{1 + \|\mathbf{h}_s\|^2}\right), \tag{4}$$

where $\gamma = \frac{N_1}{N_1 + N_2}$. The destination, by using Maximal-Ratio Combining (MRC), decodes $X_b(w_1)$ by treating $X_{a1}(w_0)$ as noise from

$$\mathbf{y}_d[1] = \mathbf{h}_s\sqrt{1 - \delta}X_b(w_1) + \mathbf{h}_s\sqrt{\delta}X_{a1}(w_0) + \mathbf{z}_d[1],$$

which is possible if

$$R_b \leq \gamma \log\left(1 + \|\mathbf{h}_s\|^2\right) - \gamma \log\left(1 + \frac{\|\mathbf{h}_s\|^2}{1 + \|\mathbf{h}_s\|^2}\right). \tag{5}$$

In order to obtain R_b in (5) we computed $\log\left(1 + (1 - \delta)\,\mathbf{h}_s^H\mathbf{\Sigma}_1^{-1}\mathbf{h}_s\right)$ where $\mathbf{\Sigma}_1 \in \mathbb{C}^{2\times 2}$ is the covariance matrix of the equivalent noise

$$\tilde{\mathbf{z}}_1 = \mathbf{h}_s\sqrt{\delta}X_{a1}(w_0) + \mathbf{z}_d[1]$$

and where the final expression follows as an application of the "matrix inversion lemma[1]". Notice that the same rate is obtained if the receiver computes the scalar $\frac{\mathbf{h}_s^H}{\|\mathbf{h}_s\|}\mathbf{y}_d[1] = \|\mathbf{h}_s\|\sqrt{1 - \delta}X_b(w_1) + \|\mathbf{h}_s\|\sqrt{\delta}X_{a1}(w_0) + Z$, $Z \sim N(0, 1)$ and decodes X_b. Finally, by assuming $\|\mathbf{h}_s\|^2 < |h_{rs}|^2$ (we will see later that this assumption is without loss of generality), Phase I is successful if (4) and (5) are satisfied.

---

[1]Matrix inversion lemma $(A + XBX^T)^{-1} = A^{-1} - A^{-1}X(B^{-1} + X^TA^{-1}X)^{-1}X^TA^{-1}$.

Phase II During this phase the relay is transmitting, i.e., $S_r = 1$ (see Fig. 1(b)). The source selects uniformly at random a message $w_2 \in [1 : M_2]$ (sent directly to the destination) and the relay forwards its estimation of w_0 from Phase I, indicated as $\widehat{w}_0$. The transmitted signals are

$$X_s[2] = X_c(w_2),$$
$$X_r[2] = X_{a2}\left(\widehat{w}_0\right).$$

The destination uses MRC and applies successive decoding based on

$$\mathbf{y}_d[2] = \mathbf{h}_s X_c(w_2) + \mathbf{h}_r X_{a2}\left(\widehat{w}_0\right) + \mathbf{z}_d[2].$$

In particular, it first decodes w_0 by using the received signal from both phases and by assuming that $\widehat{w}_0 = w_0$; this is true given the rate constrains found for Phase I. It then decodes $X_c(w_2)$, after having subtracted the contribution of its estimated w_0. Successful decoding is possible if

$$R_a \le (1 - \gamma) \log \left(1 + \frac{\|\mathbf{h}_r\|^2 + \|\mathbf{h}_r\|^2 \|\mathbf{h}_s\|^2 \left(1 - |v|^2\right)}{1 + \|\mathbf{h}_s\|^2}\right) + \gamma \log \left(1 + \frac{\|\mathbf{h}_s\|^2}{1 + \|\mathbf{h}_s\|^2}\right),$$
(6)

$$R_c \le (1 - \gamma) \log \left(1 + \|\mathbf{h}_s\|^2\right),$$
(7)

where v is defined in (2b). In order to obtain R_a in (6) we computed $\log\left(1 + \mathbf{h}_r^H \mathbf{\Sigma}_2^{-1} \mathbf{h}_r\right)$, where $\mathbf{\Sigma}_2 \in \mathbb{C}^{2 \times 2}$ is the covariance matrix of

$$\tilde{\mathbf{z}}_2 = \mathbf{h}_s X_c\left(w_2\right) + \mathbf{z}_d[2]$$

and where the final expression follows as an application of the "matrix inversion lemma". By imposing that the rate R_a is the same in both phases, that is, that (4) and (6) are equal, we get that γ should be chosen equal to γ^*

$$\gamma^* = \frac{\underline{a}}{\underline{a} + \underline{b}},$$
(8)

where $\underline{a}$ and $\underline{b}$ are defined in (2b) and (2c), respectively. Note that by the assumption $\|\mathbf{h}_s\|^2 < |h_{rs}|^2$, so we have $\underline{b} > 0$, i.e., $\underline{b} = [\underline{b}]^+$.

The rate sent directly from the source to the destination, that is, the sum of (5) and (7), is

$$R_b + R_c = \log\left(1 + \|\mathbf{h}_s\|^2\right) - \underbrace{\gamma^* \log\left(1 + \frac{\|\mathbf{h}_s\|^2}{1 + \|\mathbf{h}_s\|^2}\right)}_{\in[0,1]}.$$
(9)

Therefore the total rate decoded at the destination through the two phases is $R = R_b + R_c + R_a$ as in (2a), which implies

$$\mathsf{C} \ge R_b + R_c + R_a \ge \log(1 + \|\mathbf{h}_s\|^2) + \frac{\underline{a}\,\underline{b}}{\underline{a} + \underline{b}}.$$
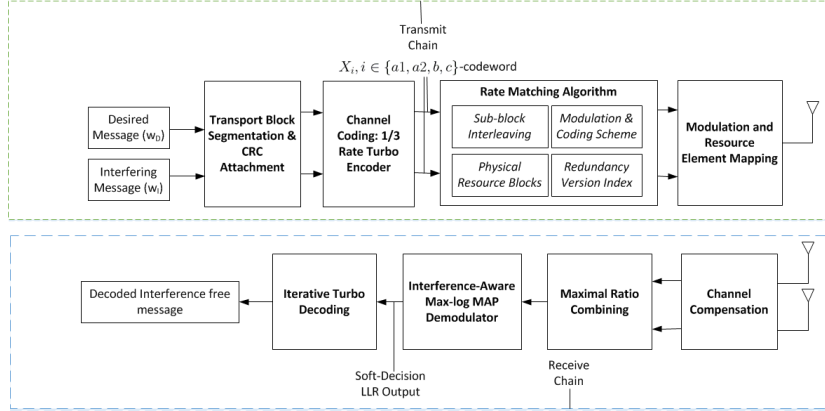(10)

Figure 2: Overall simulation block diagram for the transmit and receive chains.

as in (2a). The rate expression for R in (2a), with $[b]^+$ rather than b, holds since for $\|\mathbf{h}_s\|^2 \geq |h_{rs}|^2$ it reduces to a direct transmission from the source to the destination. Moreover, the scheme here presented for the case of 2 antennas at the destination, straightforwardly generalizes to the case when the destination is equipped with a general number n_d of antennas. It is shown that the proposed scheme is optimal to within 3.51 bits/dim, independently of the number of antennas n_d at the destination. Note that the single-antenna result in [6, Proposition 5] is obtained as a special case of Proposition 1 by setting: $|h_{ds_1}|^2 = S$, $|h_{dr_1}|^2 = I$, $|h_{rs}|^2 = C$ and $|h_{ds_2}|^2 = |h_{dr_2}|^2 = 0$. $\qquad\square$

Next we propose a practical LTE-based implementation to achieve the rate in Proposition 1.

3 Simulation Test-bench Design

The scheme described in Proposition 1 uses four Gaussian codebooks $\mathcal{C}_{a1}$, $\mathcal{C}_{a2}$, $\mathcal{C}_b$ and $\mathcal{C}_c$ to transmit the three messages w_0, w_1 and w_2. In a practical implementation, the codes would not be Gaussian, but be composed of symbols from a finite constellation. Since SIC is employed in the decoding operations both at the relay and at the destination, we need to understand the performance of these practical codes both in Gaussian and non-Gaussian noise. In particular, at the relay we need to understand the performance of $\mathcal{C}_b$ in non-Gaussian noise (first decoding step of Phase I) and of $\mathcal{C}_{a1}$ in Gaussian noise (second decoding step of Phase I); at the destination we have to understand the performance of $\mathcal{C}_{a1}$, $\mathcal{C}_{a2}$ and $\mathcal{C}_b$ in non-Gaussian noise ($\mathcal{C}_b$ in the first decoding step in Phase I and $\mathcal{C}_{a1}$, $\mathcal{C}_{a2}$ in the first decoding step in Phase II) and the performance of code $\mathcal{C}_c$ in Gaussian noise (second decoding operation in Phase II when no error propagation). In the decoding stages where a message is treated as noise, we develop a decoder that specially accounts for the fact that the overall noise is non-Gaussian. We will consider different choices for the codebooks $(\mathcal{C}_{a1}, \mathcal{C}_{a2}, \mathcal{C}_b, \mathcal{C}_c)$; for each choice, we make sure that in all the de-

6

coding stages we have a BLER below a given threshold (here set to 10^{-2} in order to have a probability of successful decoding of 0.99). This analysis will be conducted both for the case of single-antenna destination and for the case when the destination is equipped with two antennas. The question we seek to answer in the following is how close the spectral efficiency of practical codes is compared to the theoretical performance in Proposition 1.

We developed a simulation testbed using the OAI (a platform for wireless communication experimentation) software libraries in order to evaluate the performance of the aforementioned scheme with practical codes (see Fig. 2). The software platform is based on 3GPP's evolving standard of LTE which consists of the essential features of a practical radio communication system, which closely align with the standards in commercially deployed networks. Fig. 2 shows the key functional units of the simulation design. The simulations were carried out on the Downlink Shared Channel (DL-SCH), which is the primary channel for transmitting user-data (or control information) from the eNB to the UE [7]. The data messages are transported in units known as Transport Blocks (TBs) to convey the messages w_0, w_1 and w_2. The TB Size (TBS) depends on the choice of the Modulation and Coding Scheme (MCS), which describes the modulation order and the coding rate of a particular transmission.

Processing The TBs undergo a series of processing stages prior to modulation before the codeword can be mapped into the Resource Elements (REs) in the Physical DL-SCH (PDSCH). Error detection at the receiver is enabled by appending 24 Cyclic Redundancy Check (CRC) bits to the TB. The code block (comprising of the TB and of the CRC bits) has a minimum and maximum size of 40 and 6144 bits, respectively, as required by the Turbo encoder. Filler bits are added if the code block is too small in size and the code block is segmented into blocks of smaller size if the maximum size is exceeded. The subsequent bit sequence is then fed into the $1/3$ rate Turbo encoder.

Channel Coding The channel coding scheme comprises of a 1/3 rate Turbo encoder, which follows the structure of a parallel concatenated convolutional code with two 8-state constituent encoders, and one Turbo code internal interleaver [8]. A single set of systematic bits and two sets of parity bits are produced at the output of the encoder as detailed in [8].

Rate Matching The rate matching component ensures, through puncturing or repetition of the bits, that the output bits from the Turbo encoder match the available physical resources using the MCS, the Redundancy Version (RV) index and the Physical Resource Blocks (PRBs). For the numerical evaluations, an equal bandwidth allocation is chosen between the two phases of the relay strategy, i.e., the number of PRBs allocated in the first (relay listening) and second (relay transmitting) phases is the same. In other words, with reference to (8), we set $\gamma = 0.5$,

which may not be the optimal choice. The message w_0, transmitted by the source and the relay over the two phases, corresponds to two different RVs with equal resource allocations. The selection is made possible through puncturing or repetition of the bits at the output of the encoder. The Circular Buffer (CB) generates puncturing patterns depending on the allocated resources, and the sub-block interleaver (which forms part of the CB) facilitates the puncturing of the three outputs of the encoder [7]. Furthermore, the code block is concatenated if segmentation was required prior to channel coding.

Modulation and REs Mapping During this stage, complex-valued symbols are generated according to the chosen modulation scheme, i.e., QPSK, 16-QAM or 64-QAM, which are supported in LTE. In this study we will use QPSK as well as higher-order modulations such as 16-QAM and 64-QAM. In particular, we will employ the same modulation order at the source and at the relay. Such a scheme performs well when the channel quality between the relay and the destination is not much better than that of the source-destination link. However, when the relay-destination link is significantly stronger than the source-destination link, a better performance/higher spectral efficiency could be attained with higher modulation schemes at the relay.

Channel Compensation and MRC The channel compensation block is responsible for computing the Matched Filtered (MF) outputs and effective channel magnitudes of the received signal. These parameters are required for the soft-decoding of the desired message using the interference-aware demodulator. The MRC block utilizes the MF outputs to constructively add the two received signals to maximize the post-processing SNR (notice that the MRC block is not needed in the case when the destination is equipped with a single-antenna).

Interference-Aware Demodulator The demodulator comprises of a discrete constellation interference-aware receiver designed to be a low-complexity version of the max-log MAP detector. The main idea is to decouple the real and imaginary components through a simplified bit-metric using the MF output and thus reduce the search space by one complex dimension [9]. As a result, it is possible to decode the required codeword in the presence of an interfering codeword of the same (or different) modulation scheme. Thereafter, it is possible to strip out the decoded signal from the received signal and then decode the remaining signal in an interference-free channel in case of no error propagation. The generated LLRs are soft-combined in decoding w_0 at the destination at the end of Phase II, i.e., X_{a1} (received in Phase I) and X_{a2} (received in Phase II) are combined to obtain the message w_0.

8

Figure 3: SISO BLER performances of w_0, w_1 and w_2 at the destination versus different strengths of the direct source-destination link.

4 Performance Evaluation

In this section we numerically evaluate the performance of the proposed transmission strategy with different channel models. In particular, in Section 4.1 we consider the static/no-fading AWGN channel model, and in Section 4.2 we consider two frequency-selective fading models, i.e., the EPA and the ETU low-mobility LTE multipath channel models, where the corresponding fading amplitudes are characterized by a Rayleigh distribution. The transmission bandwidth of the simulated system is 5 MHz, corresponding to 25 PRBs.

4.1 AWGN Channel Model Evaluation

For the static channel model, in (1) we let $|h_{rs}|^2 = C$, $|h_{ds_1}|^2 = |h_{ds_2}|^2 = S$ (i.e., the two source-destination links are of the same strength), $|h_{dr_1}|^2 = |h_{dr_2}|^2 = I$ (i.e., the two relay-destination links are of the same strength), and we set the phase of the channel gains to some random value that is kept constant during the whole simulation. Perfect receive CSI is assumed at all nodes. For each of the decoding operations during Phases I and II, the BLER performances at the relay and destination are validated for different values of C (at the relay) and evaluated with respect to S (channel quality for the source-destination link). Furthermore, we use $\delta = \frac{1}{1+2S}$ as the superposition parameter in the SIMO scenario and $\delta = \frac{1}{1+S}$ in the SISO case, which we showed to be optimal to within a constant gap. An equal bandwidth allocation between the two phases of the strategy is also assumed, i.e., $\gamma = 0.5$.

Decoding at the relay At the end of Phase I, the relay first decodes w_1, then it strips it out from its received signal and finally decodes w_0. The maximum source-relay channel strength for which the message w_1 can be successfully decoded at
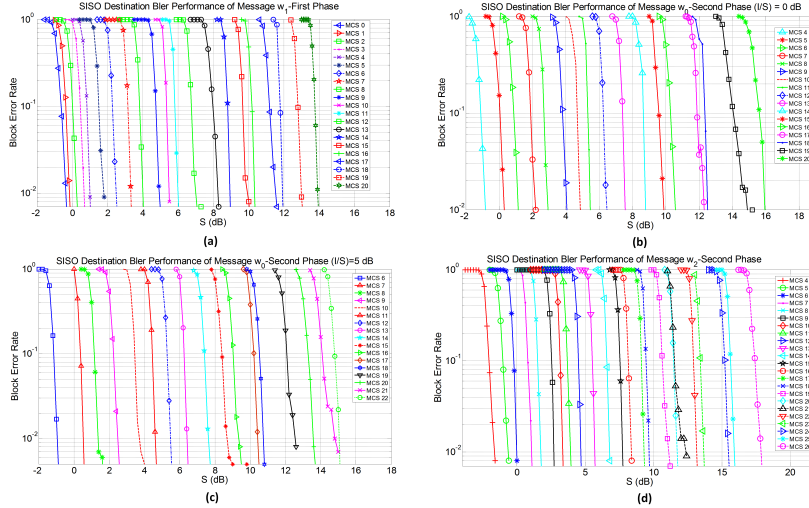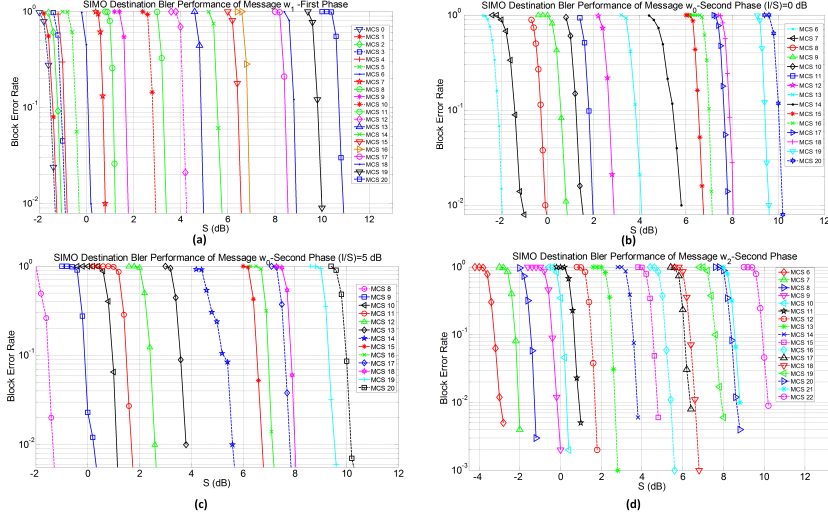
Figure 4: SIMO BLER performances of w_0, w_1 and w_2 at the destination versus different strengths of the direct source-destination link.

a BLER of 5×10^{-4} at the relay is denoted as C_{X_b}. Thereafter, the message w_1 is stripped out and the relay decodes the message w_0 on an interference-free link. Error propagation, which results from feeding back incorrectly decoded symbols, is not considered here. The reason is that we consider a coded system with CRC, which ensures near perfect decoding of the transmitted message; any residual error at the output of the CRC occurs with a very low probability and thus we neglect these errors here. The corresponding maximum quality channel strength for successfully decoding message w_0 is denoted as $C_{X_{a1}}$. In order to have successful decoding operations (of both w_0 and w_1) at the relay at the end of Phase I, we require a value of C such that the BLER $\leq (\Pr[X_b] + \Pr[X_{a1}]) \leq 10^{-3}$. and that is shown in the third column of Tables 1 (SISO) and 3 (SIMO) for $I/S = 0$ dB and Tables 2 (SISO) and 4 (SIMO) for the $I/S = 5$ dB case. At the beginning of Phase II, the message w_0 is re-encoded and forwarded by the relay to the destination.

Decoding at the destination   The SISO and SIMO BLER performance of w_1 for Phase I, are shown in Fig. 3(a) and Fig. 4(a), respectively, for MCS values ranging in the interval $[0:20]$ to encompass 16-QAM and 64-QAM transmissions with different code rates. Similarly for Phase II, the BLER performances of w_0 are shown in Fig. 3(b) (SISO) and Fig. 4(b) (SIMO) for $I/S = 0$ dB and in Fig. 3(c) (SISO) and Fig. 4(c) (SIMO), for $I/S = 5$ dB. Finally, Fig. 3(d) (SISO) and Fig. 4(d) (SIMO) show the BLER performances of the third transmitted message w_2, at the end of Phase II, which is decoded after the perfect stripping of w_0 once it has been successfully decoded. It is worth noting that in our model, the relay-destination link is assumed to be stronger than the source-destination link so that using the relay indeed boosts the rate performance with respect to direct transmission.

10

Table 1: MCS mapping for each decoding operation with $I/S = 0$ dB for a SISO scheme.

Phase I - X_b				Phase II - (X_{a1}, X_{a2})		Phase II - X_c		Theory	Practical	Theory BS	Practical BS
MCS	S_{X_b} [dB]	C [dB]	TBS [bits]	MCS	TBS [bits]	MCS	TBS [bits]	Rate [bits/dim]	Rate [bits/dim]	Rate [bits/dim]	Rate [bits/dim]
0	-0.22	1.25	680	5	2216	6	2600	1.06	0.89	0.60	0.53
1	-0.02	1.25	904	5	2216	6	2600	1.09	0.93	0.63	0.53
2	0.39	1.25	1096	5	2216	7	2600	1.13	1.04	0.67	0.63
3	0.80	2.02	1416	5	2216	7	3112	1.23	1.10	0.71	0.63
4	1.15	2.02	1800	6	2600	7	3112	1.27	1.22	0.75	0.63
5	1.95	3.51	2216	7	3112	9	2216	1.50	1.52	0.84	0.80
6	2.66	4.17	2600	8	3496	9	4008	1.63	1.64	0.92	0.80
7	3.43	4.83	3112	9	4008	10	4008	1.80	1.81	1.03	0.79
8	4.11	6.59	3496	9	4008	12	4968	2.05	2.02	1.12	0.98
9	5.13	6.59	4008	10	4008	13	5736	2.24	2.24	1.25	1.11
10	5.58	6.59	4008	11	4392	13	5736	2.30	2.30	1.33	1.11
11	6.13	8.64	4392	12	4968	14	6456	2.60	2.57	1.41	1.25
12	7.40	9.54	4968	13	5736	15	7224	2.92	2.92	1.56	1.37
13	8.41	11.11	5736	14	6456	16	7736	3.26	3.24	1.75	1.46
14	9.01	13.40	6456	15	7224	17	7736	3.61	3.48	1.86	1.45
15	10.25	13.40	7224	16	7736	18	7992	3.88	3.73	2.02	1.49
16	10.45	15.75	7736	16	7736	19	9144	4.12	4.00	2.08	1.69
$17^{\dagger}$	11.79	15.75	7736	17	7736	20	9912	$4.44^{\dagger}$	$4.13^{\dagger}$	2.28	1.82
18	11.99	15.75	7992	17	7736	21	10680	4.46	4.29	2.34	1.96
19	13.24	16.67	9144	19	9144	22	11448	4.84	4.84	2.52	2.08
$20^{\star}$	14.04	18.2	9912	19	9144	23	12576	5.16	$5.14^{\star}$	2.67	$2.28^{\star}$

Table 2: MCS mapping for each decoding operation with $I/S = 5$ dB for a SISO scheme.

Phase I - X_b				Phase II - (X_{a1}, X_{a2})		Phase II - X_c		Theory	Practical	Theory BS	Practical BS
MCS	S_{X_b} [dB]	C [dB]	TBS [bits]	MCS	TBS [bits]	MCS	TBS [bits]	Rate [bits/dim]	Rate [bits/dim]	Rate [bits/dim]	Rate [bits/dim]
0	-0.22	6.01	680	5	2600	6	2600	1.49	1.03	0.79	0.90
1	-0.02	6.01	904	5	2600	6	2600	1.51	1.07	0.91	1.04
2	0.39	6.01	1096	5	2600	7	3112	1.55	1.19	0.91	1.04
3	0.80	8.08	1416	6	3112	7	3112	1.82	1.30	0.91	1.17
4	1.15	8.08	1800	6	3112	7	3112	1.85	1.37	1.02	1.17
5	1.95	8.08	2216	7	3496	9	4008	1.96	1.66	1.02	1.30
6	2.66	9.20	2600	8	3496	9	4008	2.15	1.73	1.15	1.39
7[†]	3.43	11.22	3112	9	4008	10	4008	**2.49**[†]	**1.81**[†]	1.23	1.39
8	4.11	11.22	3496	10	4008	12	4968	2.58	2.09	1.23	1.63
9	5.13	11.22	4008	11	4392	13	5736	2.72	2.39	1.45	1.63
10	5.58	11.22	4008	12	5736	13	5736	2.78	2.51	1.45	1.76
11	6.13	13.70	4392	12	4968	14	6456	3.12	2.69	1.57	1.88
12	7.40	13.70	4968	13	5736	15	7224	3.38	3.03	1.70	2.21
13	8.41	13.70	5736	14	6456	16	7736	3.55	3.36	2.00	2.21
14	9.01	15.34	6456	15	7224	17	7736	3.85	3.48	2.00	2.19
15	10.25	16.60	7224	16	7736	18	7992	4.26	3.73	2.00	2.19
16	10.34	18.20	7736	16	7736	19	9144	4.51	4.00	2.00	2.34
17	11.79	18.20	7736	17	7992	20	9912	4.74	4.13	2.15	2.34
18	11.99	18.20	7992	17	7992	21	10680	4.76	4.17	2.15	2.34
19	13.24	18.20	9144	19	9144	22	11448	5.02	4.96	2.15	2.34
20[★]	14.04	21.00	9912	19	9912	23	12576	5.52	**5.39**[★]	2.42	**2.63**[★]

Table 3: MCS mapping for each decoding operation with $I/S = 0$ dB for a SIMO scheme.

Phase I - X_b				Phase II - (X_{a1}, X_{a2})		Phase II - X_c		Theory	Practical	Theory BS	Practical BS
MCS	S [dB]	C [dB]	TBS [bits]	MCS	TBS [bits]	MCS	TBS [bits]	Rate [bits/dim]	Rate [bits/dim]	Rate [bits/dim]	Rate [bits/dim]
0	-1.26	3.56	680	8	3112	8	3496	1.46	1.19	0.75	0.70
1	-1.18	3.56	904	7	3112	9	4008	1.46	1.30	0.75	0.70
2	-0.93	4.15	1096	7	3112	9	4008	1.53	1.34	0.79	0.80
3	-0.81	4.15	1416	7	3112	9	4008	1.55	1.39	0.80	0.80
4	-0.69	4.82	1800	7	3112	9	4008	1.63	1.45	0.83	0.80
5	-0.25	5.88	2216	8	3496	9	4008	1.78	1.58	0.92	0.80
6†	0.43	7.02	2600	8	3496	11	4392	1.98†	1.71†	1.02	0.80
7	0.86	7.02	3112	9	4008	11	4392	2.05	1.87	1.06	0.86
8	1.27	7.93	3496	10	4008	12	4968	2.20	2.15	1.13	0.97
9	1.89	9.54	4008	11	4968	13	5736	2.44	2.26	1.01	1.12
10	3.01	9.54	4008	13	5736	14	6456	2.64	2.63	1.37	1.24
11	3.45	9.54	4392	13	5736	14	6456	2.71	2.70	1.41	1.24
12	4.33	11.59	4968	14	6456	15	7224	3.07	3.03	1.60	1.38
13	5.02	12.10	5736	14	6456	16	7736	3.25	3.24	1.69	1.45
14	5.84	12.10	6456	14	6456	17	7736	3.41	3.36	1.56	1.46
15	6.64	14.00	7224	15	7224	18	7992	3.76	3.65	1.96	1.49
16	7.00	15.58	7736	15	7224	19	9144	3.96	3.92	2.08	1.49
17	8.60	16.20	7736	19	9144	20	9912	4.38	4.36	2.29	1.68
18	8.96	18.20	7992	19	9144	21	10680	4.61	4.52	2.43	1.68
19	10.10	18.20	9144	20	9912	21	10680	4.89	4.84	2.56	1.94
20*	11.02	18.20	9912	20	9912	22	11448	5.10	5.09*	2.36	1.93*

Table 4: MCS mapping for each decoding operation with $I/S = 5$ dB for a SIMO scheme.

Phase I - X_b				Phase II - (X_{a1}, X_{a2})		Phase II - X_c		Theory	Practical	Theory BS	Practical BS
MCS	S [dB]	C [dB]	TBS [bits]	MCS	TBS [bits]	MCS	TBS [bits]	Rate [bits/dim]	Rate [bits/dim]	Rate [bits/dim]	Rate [bits/dim]
0	-1.26	7.93	680	9	4008	8	3496	1.88	1.33	1.34	1.17
1	-1.18	9.54	904	9	4008	9	4008	2.03	1.45	1.44	1.17
2	-1.06	9.54	1096	9	4008	9	4008	2.06	1.48	1.46	1.17
3	-0.81	9.54	1416	9	4008	9	4008	2.08	1.53	1.47	1.30
4	-0.69	9.54	1800	9	4008	9	4008	2.10	1.60	1.48	1.30
5	-0.25	11.59	2216	9	4008	9	4008	2.32	1.66	1.64	1.30
6	0.43	11.59	2600	10	4008	11	4392	2.43	1.79	1.70	1.39
$7^{\dagger}$	0.86	12.10	3112	10	4008	11	4392	$2.54^{\dagger}$	$1.87^{\dagger}$	1.77	1.39
8	1.27	13.40	3496	11	4392	12	4968	2.70	2.21	1.89	1.39
9	1.89	14.00	4008	12	4968	13	5736	2.86	2.40	1.98	1.42
10	3.01	14.00	4008	13	5736	14	6456	3.08	2.51	2.09	1.42
11	3.45	14.00	4392	13	5736	14	6456	3.17	2.57	2.13	1.62
12	4.33	16.20	4968	13	5736	15	7224	3.51	3.03	2.36	1.62
13	5.02	18.20	5736	14	6456	16	7736	3.79	3.24	2.55	1.88
14	5.84	18.20	6456	15	7224	17	7736	3.98	3.48	2.64	2.00
15	6.64	18.20	7224	15	7224	18	7992	4.17	3.65	2.72	2.00
16	7.00	18.20	7736	16	7736	19	9144	4.25	4.00	2.75	2.20
17	8.60	18.20	7736	19	9144	20	9912	4.63	4.36	2.90	2.35
18	8.96	18.20	7992	19	9144	21	10680	4.70	4.53	2.93	2.45
19	10.10	18.20	9144	20	9912	22	11448	4.95	4.96	3.03	2.64
$20^{\star}$	11.01	21.00	9912	21	10680	23	12576	5.42	$5.39^{\star}$	3.32	$2.73^{\star}$

The results in Fig. 3, Fig. 4, Tables 1 and 3 ($I/S = 0$ dB) and Tables 2 and 4 ($I/S = 5$ dB) were generated as follows. From Fig. 3(a) and Fig. 4(a) we considered a decoding probability of BLER $= 3 \times 10^{-3}$ and, for each value of the MCS of X_b (first column of Tables 1, 2, 3 and 4), we selected the corresponding value of S (second column of Tables 1, 2, 3 and 4), in order to correspond to a BLER $\leq (\Pr[\mathrm{X_b}] + \Pr[\mathrm{X_{a1}, X_{a2}}] + \Pr[\mathrm{X_c}]) \leq 10^{-2}$.. Thereafter, for each value of the ratio I/S, we selected the MCS of (X_{a1}, X_{a2}) which, for each value of S (second column of Tables 1, 2, 3 and 4), allowed to achieve a BLER $\leq 3 \times 10^{-3}$. These MCS values are reported in the sixth column of Tables 1, 2, 3 and 4. Similarly, we proceeded in selecting the MCS of X_c (eighth column of Tables 1, 2, 3 and 4). The TBSs of each MCS (at the source and at the relay), as defined by the 3GPP in the LTE standard [10], are also reported in Tables 1, 2, 3 and 4.

Comparison with theoretical performance One of our major goals in this work is to compare the theoretical and practical spectral efficiency performance of the proposed strategy. To this end, in the ninth column of Tables 1, 2, 3 and 4, the theoretical rate is shown and computed as follows. For the SISO case, we first computed the "theoretical" value of C by inverting [6, eq.(42)] with $\gamma = 0.5$ (in order to account for the fact that the duration of the two phases is equal) and then we used the values of (S, I, C) to compute [6, eq.(37)]. Similarly, for the SIMO case we inverted (8) in order to obtain the "theoretical" value of C and then we used the values of (S, I, C) to compute (2). The spectral efficiency of our practical scheme (tenth column of Tables 1, 2, 3 and 4) was determined by using the ratio of the TBS (useful message length) with respect to the number of soft-bits (G-codeword size) together with the modulation order, which does not include the overhead bits such as the cyclic prefix, pilots and control channel information (PDCCH symbols). In particular,

$$ R = \frac{\mathrm{TBS}(X_b) + \mathrm{TBS}\,(X_{a1}, X_{a2}) + \mathrm{TBS}(X_c)}{\left(\frac{\mathrm{G_1}}{\mathrm{Q_{mod1}}} + \frac{\mathrm{G_2}}{\mathrm{Q_{mod2}}} \right)} \text{ bits/dim,} \qquad (11) $$

where $\mathrm{G_1}$ is the number of soft-bits used to decode (X_b, X_{a1}) and $\mathrm{G_2}$ to decode (X_{a2}, X_c), and $\mathrm{Q_{mod1}}$ and $\mathrm{Q_{mod2}}$ are the corresponding modulation orders.[2]

Simulation results [3] For the SISO case, from Tables 1 and 2, the maximum difference between the theoretical rate in [6, eq.(37)] and the achieved rate by the proposed scheme (highlighted in boldface) is of 0.36 bits/dim when $I/S = 0$ dB and of 0.83 bits/dim when $I/S = 5$ dB. Similarly, from Tables 3 and 4, the maximum difference between the theoretical rate and the achieved rate (also highlighted in boldface) by the proposed scheme is of 0.49 bits/dim when $I/S = 0$ dB and of

---

[2]TBS is the number of information bits, G is the number of coded bits and $\mathrm{Q} \equiv \log M$ where M is the modulation order.

[3]In Tables 1-4 with a † we indicate the MCS at which the maximum difference between the theoretical and the practical rates occurs.

0.79 bits/dim when $I/S = 5$ dB. These rate gaps between theory and practice can be mostly attributed to two key factors: (i) the TBs used are of finite length, differently from the theoretical assumption of infinite block length and (ii) the channel inputs are drawn from a discrete constellation, rather than from Gaussian codebooks as assumed in the theoretical analysis. Furthermore, the fact that the difference is higher when $I/S = 5$ dB than when $I/S = 0$ dB is due to the fact that when the ratio I/S increases it becomes more critical to choose higher MCS values for the relay in order to fully exploit the strength of the relay-destination link. Adapting the modulation order and the number of PRBs across different rounds may reduce the theoretical and practical performance gap. Moreover, we also remark that the difference between theoretical and practical rates might be decreased by performing an optimization of the parameters δ (superposition factor) and γ (fraction of time the relay listens to the channel) in the interval $[0, 1]$, instead of considering them as fixed values (which has been deemed out of the scope of this study).

The practical rates of the SIMO scheme outperform those of the SISO scheme, exploiting the benefits of the beamforming gain arising from the use of two antennas at the destination. Consider the case when the strengths of the source-destination and relay-destination links are the same and $S \approx= 9$ dB: the SISO UE operates at an MCS of 14 (16-QAM), while for the approximate same value of S the SIMO operates at an MCS of 18 (64-QAM), thus taking advantage of a higher modulation scheme while being 1.04 bits/dim more spectrally efficient than the SISO scheme.

Baseline relay scheme For comparisons with existing relay structures, we also considered a Baseline Scheme (BS), which mimics the relay structure of today's LTE networks, where the UE does not have a direct connection with the eNB, i.e., the source-destination link is absent and the eNB can only communicate with the UE through the relay. For both the SISO case (last two columns of Tables 1-2) and the SIMO scenario (last two columns of Tables 3-4), the BS practical rates are compared to the theoretical ones [4]. The theoretical capacity is given by:

$$R_{\text{Theor}-\text{BS}} = \min\{\gamma \log(1 + C), (1 - \gamma) \log(1 + \alpha I)\},$$

with $\alpha = 1$ in the SISO case, while $\alpha = 2$ in the SIMO case; C is the "theoretical" value of the strength of the source-relay link (i.e., the one previously computed when the source-destination link is not absent by reversing [6, eq.(42)] for the SISO case and (8) for the SIMO case with $\gamma = 0.5$); the optimal theoretical γ is obtained by equating the two terms within the $\min$, i.e.,

$$\gamma = \frac{\log (1 + \alpha I)}{\log (1 + \alpha I) + \log (1 + C)}.$$

---

[4]In Tables 1-4 with a $\star$ we indicate the MCS at which the maximum difference between the rates of the practical and baseline schemes occurs.

16

Table 5: LTE delay spread profile.

	Extended Pedestrian A			Extended Typical Urban	
	Excess Tap Delay [ns]	Relative Power [dB]		Excess Tap Delay [ns]	Relative Power [dB]
1	0	0.0	1	0	-1.0
2	30	-1.0	2	50	-1.0
3	70	-2.0	3	120	-1.0
4	90	-3.0	4	200	0.0
5	110	-8.0	5	230	0.0
6	190	-17.2	6	500	0.0
7	410	-20.8	7	1600	-3.0
-	-	-	8	2300	-5.0
-	-	-	9	5000	-7.0

In the SISO case, from Tables 1 and 2, we also notice that the maximum difference (indicated in boldface) between the practical rates and the practical BS rates is of 2.87 bits/dim (factor of 2.58) and of 2.76 bits/dim (factor of 2.22), respectively. In the SIMO case, as seen in Tables 3 and 4, the maximum difference (indicated in boldface) in spectral efficiency between the practical strategy and the BS rates is of 3.15 bits/dim (factor of 2.79) for $I/S = 0$ dB, and of 2.67 bits/dim (factor of 2.14) for $I/S = 5$ dB, which is a significant improvement in spectral efficiency of the cooperative relay strategy over the basic scheme. The fact that the difference is higher when $I/S = 0$ dB than when $I/S = 5$ dB is due to the fact that when the ratio I/S is small, the presence of the source-destination link plays a significant role in the rate performance.

4.2 LTE Channel Model Evaluation

The AWGN channel modeling of the proposed relay strategy represents an idealistic scenario. In an effort to model a practical scenario, we evaluate the spectral efficiency of the strategy using two well-known low mobility frequency-selective channel models defined by the 3GPP, i.e., the EPA model and the ETU model. In particular, we focus on the scenario where the destination is equipped with two antennas (SIMO). Table 5 shows the power delay profile of the two channel models where the relative amplitude and delay of each multipath component are given [11]. The EPA and ETU models consist of seven and nine discrete multipath components, each with a coherence bandwidth of 2.43 MHz and 0.2 MHz, respectively. The amplitude distribution for each tap in the EPA and ETU models is described by a Rayleigh fading process. The complex channel coefficients for both the source-destination (h_{ds_1} and h_{ds_2}) and relay-destination (h_{dr_1} and h_{dr_2}) links are generated according to the generalized channel transfer function (in the
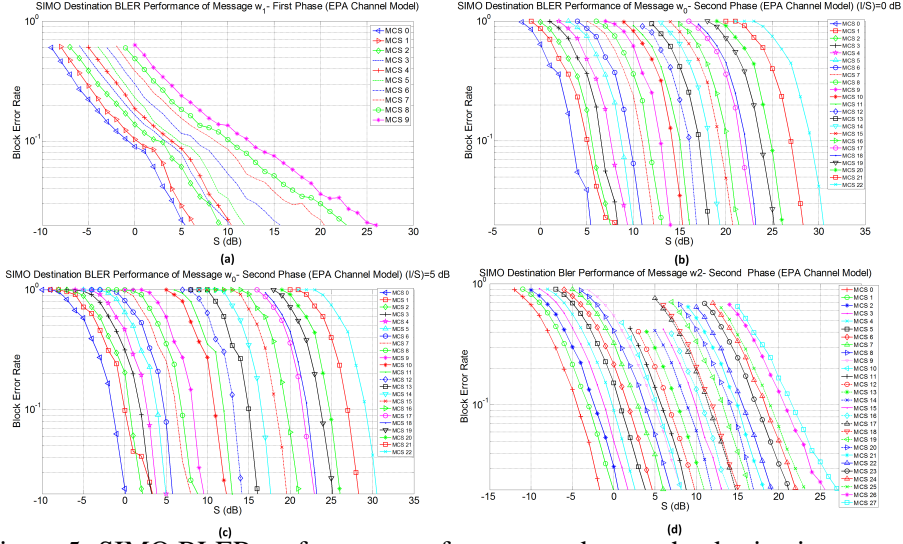
Figure 5: SIMO BLER performances of w_0, w_1 and w_2 at the destination versus different strengths of the direct source-destination link for the EPA channel model. frequency domain)

$$h_i = \sum_{l=1}^{L} \alpha_l \exp\left(-j2\pi\tau_l n f_{sub}\right), \tag{12}$$

where $i = [1 : 300]$ represents the subcarrier index for a bandwidth of 5 MHz, α_l represents the complex path amplitude, l is the path index, τ_l is the path delay and f_{sub} represents the periodic subcarrier spacing of 15 kHz (as defined in LTE) [7]. We further assume a zero doppler shift for both channel models in line with the low mobility assumption of the destination (UE). An analytical analysis of the proposed scheme on a fading channel, would involve an evaluation of the achievable rate under a given information outage probability, which would hold for the infinite block length and block-fading channel case. This would be performed by extending (2a)-(2c) to a vector channel with channel coefficients governed by the statistics of the EPA and ETU models and evaluating the achievable rates at which we obtain the desired outage probability. The latter could be used as a comparison for what is achievable with the proposed coding schemes with finite length blocks. We leave this analysis for future work and proceed here by comparing the rate of the proposed scheme with the BS. The point of this comparison is to show the rate advantage of our scheme in realistic channel models.

The analysis is as for the AWGN case, except for the following. Due to the poor BLER performance of the LTE channel models at 10^{-2} during Phase I, it was a challenge to achieve the target BLER at reasonable SNR values for higher MCSs, with an interfering codeword from the same discrete constellation. Hence, it was decided to relax the BLER constraint to 3.33×10^{-2} (and compute the corresponding spectral efficiency) such that BLER $\leq (\Pr[X_b] + \Pr[X_{a1}, X_{a2}] + \Pr[X_c]) \leq$
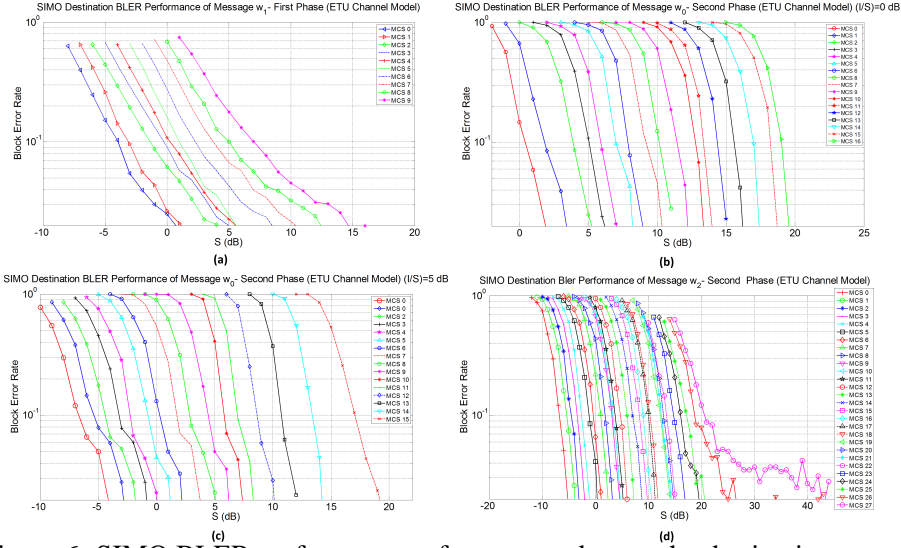
Figure 6: SIMO BLER performances of w_0, w_1 and w_2 at the destination versus different strengths of the direct source-destination link for the ETU channel model.

10^{-1} focusing on MCS values from 0 to 9 (QPSK), as H-ARQ procedures are enabled at this particular target BLER in LTE.

The results in Fig. 5 and Tables 6 and 7[5] show the results of the relay strategy using the EPA channel model. The performance of the ETU channel model (presented in Fig. 6 and Tables 8 and 9) has also been investigated. In the case of the EPA channel, from Tables 6 and 7, we observe that the maximum difference between the practical strategy and the BS rates (highlighted in boldface) is of 2.20 bits/dim for $I/S = 0$ dB and of 1.71 bits/dim for $I/S = 5$ dB. In the case of the ETU channel model, as seen in Tables 8 and 9, the maximum difference in spectral efficiency between the practical strategy and the BS rates (highlighted in boldface) is 1.50 bits/dim for $I/S = 0$ dB and 1.29 bits/dim for $I/S = 5$ dB. The difference in spectral efficiency for the practical LTE channel model is noticeably less than the AWGN SIMO case, highlighting degrading effects of the multipath on the proposed relay strategy. Nonetheless, even for these two practically relevant LTE channel models, the proposed strategy still provides remarkable improvements in spectral efficiency over the basic BS.

5   Conclusions

In this report, we designed a practical transmission strategy for the Gaussian half-duplex relay channel by using codes as in the LTE standard and by running simulations on an LTE test bench. The scheme uses superposition encoding, decode-and-forward relaying and sequential interference cancellation in order to

---

[5]In Tables 6-9 with a ⋆ we indicate the MCS at which the maximum difference between the rates of the practical and baseline schemes occurs.

Table 6: MCS mapping for each decoding operation with $I/S = 0$ dB for the EPA model.

Phase I - X_b			Phase II - (X_{a1}, X_{a2})		Phase II - X_c		Practical	Practical BS
MCS	S [dB]	TBS [bits]	MCS	TBS [bits]	MCS	TBS [bits]	Rate [bits/dim]	Rate [bits/dim]
0	4.60	680	1	904	7	3112	0.76	0.49
1	5.56	904	1	904	7	3112	0.80	0.49
2	8.50	1096	4	1800	12	4968	1.29	0.79
3	9.12	1416	4	1800	12	4968	1.33	0.79
4	9.55	1800	5	2216	13	5736	1.59	0.91
5	10.93	2216	7	3112	14	6456	1.92	1.02
6	14.20	2600	10	4008	17	7736	2.33	1.23
7	18.93	3112	14	6456	23	12576	3.60	2.00
8	21.22	3496	16	7736	24	13536	4.03	2.15
$9^\star$	24.02	4008	19	9144	26	15264	$4.62^\star$	$2.42^\star$

Table 7: MCS mapping for each decoding operation with $I/S = 5$ dB for the EPA model.

Phase I - X_b			Phase II - (X_{a1}, X_{a2})		Phase II - X_c		Practical	Practical BS
MCS	S [dB]	TBS [bits]	MCS	TBS [bits]	MCS	TBS [bits]	Rate [bits/dim]	Rate [bits/dim]
0	4.60	680	5	2216	7	3112	0.97	0.91
1	5.56	904	6	2600	7	3112	1.08	1.02
2	8.50	1096	9	4008	12	4968	1.64	1.23
3	9.12	1416	9	4008	12	4968	1.69	1.23
4	9.55	1800	10	4008	13	5736	1.88	1.27
5	10.93	2216	10	4008	14	6456	2.06	1.45
6	14.20	2600	13	5736	17	7736	2.61	2.00
7	18.93	3112	15	7224	23	12576	3.73	2.42
8	21.22	3496	17	7736	24	13536	4.03	2.51
$9^\star$	24.02	4008	19	9144	26	15264	$4.62^\star$	$2.91^\star$

Table 8: MCS mapping for each decoding operation with $I/S = 0$ dB for the ETU model.

Phase I - X_b			Phase II - (X_{a1}, X_{a2})		Phase II - X_c		Practical	Practical BS
MCS	S [dB]	TBS [bits]	MCS	TBS [bits]	MCS	TBS [bits]	Rate [bits/dim]	Rate [bits/dim]
0	0	680	0	680	5	2216	0.58	0.35
1	0.25	904	0	680	6	2600	0.68	0.41
2	2.73	1096	1	904	8	3496	0.89	0.55
3	3.85	1416	2	1096	9	4008	1.06	0.64
4	4.51	1800	2	1096	9	4008	1.19	0.70
5	4.94	2216	3	1416	11	4392	1.30	0.70
6	7.40	2600	5	2216	14	6456	1.83	1.02
7	9.19	3112	7	3112	15	7224	2.19	1.15
8	11.72	3496	9	4008	19	9144	2.71	1.45
9⋆	14.05	4008	12	4968	21	10680	**3.20⋆**	**1.67⋆**

Table 9: MCS mapping for each decoding operation with $I/S = 5$ dB for the ETU model.

Phase I - X_b			Phase II - (X_{a1}, X_{a2})		Phase II - X_c		Practical	Practical BS
MCS	S [dB]	TBS [bits]	MCS	TBS [bits]	MCS	TBS [bits]	Rate [bits/dim]	Rate [bits/dim]
0	0	680	5	2216	5	2216	0.83	0.70
1	0.25	904	5	2216	6	2600	0.93	0.79
2	2.73	1096	7	3112	8	3496	1.25	1.02
3	3.85	1416	8	3496	9	4008	1.45	1.15
4	4.51	1800	9	4008	11	4392	1.66	1.15
5	4.94	2216	9	4008	11	4392	1.73	1.23
6	7.40	2600	10	4008	14	6456	2.12	1.45
7	9.19	3112	11	4392	15	7224	2.40	1.82
8	11.72	3496	13	5736	19	9144	2.99	2.00
9⋆	14.05	4008	14	6456	21	10680	**3.43⋆**	**2.15⋆**

send three messages in two time slots from a source to a destination with the help of a relay (which forwards one of the three messages). Comparisons between the theoretical achievable rate with (point-to-point capacity achieving) Gaussian codes and the rate achieved in a practical scenario were provided for a BLER of 10^{-2} for both the single-antenna and two-antenna cases at the destination. The use of multiple antennas at the destination also highlighted the spectral efficiency gains that can be achieved. Furthermore, a baseline scheme was also considered for performance comparisons. The rate performance of this scheme, which mimics the topology of existing relay networks in today's wireless networks, was shown to be inferior to that of the proposed scheme, implying that physical layer cooperation brings about throughput gains. Finally, the half-duplex relay strategy was proven to provide robust spectral efficiency gains over the proposed baseline scheme in two well-known LTE channel models, namely the EPA and ETU models. This work shows strong promise to be deployed in upcoming release standards of LTE as well as 5G systems with respect to advanced relay architectures. Future work would include the investigation of resource allocation strategies for dynamic bandwidth assignment. In this work we considered equal duration of the two phases and a fixed value for the superposition factor; for inclusion in real-time systems, these parameters have to be adaptive. More general dimensioning of resources can be made over H-ARQ rounds. Higher-order MIMO configurations can be considered at the relay and source as well.

References

[1] A. Nosratinia, T. Hunter, and A. Hedayat, "Cooperative communication in wireless networks," *IEEE Commun. Mag.*, vol. 42, no. 10, pp. 74–80, Oct. 2004.

[2] T. M. Cover and A. A. E. Gamal, "Capacity Theorems for the Relay Channel," *IEEE Trans. Info. Theory*, vol. 25, no. 5, pp. 572–584, Sept. 1979.

[3] Third Generation Partnership Project, "Relay architectures for E-UTRA (LTE-Advanced)(Release 9)," 3GPP, Tech. Rep. 3GPP TR 36.806 v2.0.0, Feb. 2010.

[4] ——, "Further advancements for E-UTRA physical layer aspects(Release 9)," 3GPP, Tech. Rep. 3GPP TR 36.814 v9.0.0, Mar. 2010.

[5] R. Thomas, M. Cardone, R. Knopp, D. Tuninetti, and B. T. Maharaj, "An LTE implementation of a Novel Strategy for the Gaussian Half-Duplex Relay Channel," in *IEEE ICC (2015)*, Jun. 2015, pp. 2209–2214.

[6] M. Cardone, D. Tuninetti, R. Knopp, and U. Salim, "On the Gaussian Half-Duplex Relay Channel," *IEEE Trans. Info. Theor.*, vol. 60, no. 5, pp. 2542–2562, May 2014.

[7] S. Sesia, I. Toufik, and M. Baker, *LTE The UMTS Long Term Evolution: From Theory to Practice*, 2nd ed.   Wiley, 2011.

[8] Third Generation Partnership Project, "Multiplexing and channel coding (Release 11)," 3GPP, Tech. Rep. 3GPP TS 36.212 v11.3.0, Jun. 2013.

[9] R. Ghaffar and R. Knopp, "Spatial Interference Cancellation Algorithm," in *IEEE Wireless Commun. and Networking Conf.*, Apr. 2009, pp. 1–5.

[10] Third Generation Partnership Project, "Phyisical Layer Procedures (Release 11)," 3GPP, Tech. Rep. 3GPP TS 36.213 v11.3.0, Jun. 2013.

[11] ——, "Base Station (BS) radio transmission and reception," 3GPP, Tech. Rep. 3GPP TR 36.104 v8.2.0, May 2008.